Master's Thesis of Science in Agriculture

Study for the beneficial effect and application of phytochemicals

파이토케미칼의 유용 효능과 응용 방법에 대한 연구

August 2017

Hee-jung Lim

Department of International Agricultural Technology
Graduate School of International Agricultural Technology
Seoul National University

Abstract

To characterize inhibitory activities of phenolic compounds against NS2B-NS3 protease of ZIKA virus (ZIKV NS2B-NS3^{pro}) and their structure activity relationship, in this study, ZIKV NS2B-NS3^{pro} was expressed in *E. coli* BL21(DE3) as 35 kDa protein. The enzyme was displayed a K_m of 26.3 μM with fluorogenic peptide Dabcyl-KTSAVLQSGFRKME-Edan, and purified ZIKV NS2B-NS3^{pro} was used for inhibition and kinetic assays with twenty-two phenolic compounds. These phenolic compounds inhibited the activity of ZIKV NS2B-NS3^{pro} by 6.2% to 87.9%. The IC_{50} of seven phenolic compounds ranged from 22.2 ± 0.2 to 112.0 ± 5.5 μM. Myricetin showed mixed type inhibitory pattern against ZIKV NS2B-NS3^{pro} protease with IC_{50} values of 22.2 ± 0.2 μM and K_i value of 8.9 ± 1.9 μM. Relationships between chemical structures and inhibitory activities against ZIKV NS2B-NS3^{pro} can be further explored to develop highly selective inhibitors against ZIKV NS2B-NS3^{pro}.

Solubility plays a key role of bioavailability in human body. Rubusoside is a steviol glycoside sweetener in herbal tea and widely known for enhancing solubility in water. Stevioside, also a steviol glycoside sweetener, was commonly cultivated in many countries compared with rubusoside. β -galactosidase from *Thermus thermophilus* presented hydrolytic activity on β -1,2 linkage of stevioside, and can convert from stevioside to rubusoside. In this study, to industrialize production of rubusoside, firstly, β-galactosidase from *T. thermophilus* was expressed in *E. coli* BL21(DE3)plysS using lactose induction. Enzyme immobilization has several advantages for enzyme reaction.

Immobilized enzyme could be repeatedly used without another method of separation and the decrease in its activity was not largely observed. Sodium alginate was used for enzyme immobilization. Stevioside conversion for free enzyme and immobilized enzyme were shown over 77%. Enzyme reaction was carried out in the vertical double-jacket glass column reactors thermostatted at 70°C for continuous reaction. Immobilized enzyme was stable for 31 days in double-jacket glass column reactors and activity of immobilized enzyme was remained 51.4% after 31 days.

Key words: Myricetin, phenolic compounds, Protease, Zika virus, NS2B-NS3 protease, Rubusoside, Stevioside, *Thermus thermophilus*, Fermentation

Student number : 2015-22426

Contents

Chapter 2. Production of rubusoside from stevioside using β-galactosidase from *Thermus thermophilus*

List of tables

List of figures

Chapter 1.

Inhibitory effect of phenolic compounds against ZIKA virus NS2B-NS3 protease and their structure activity relationship

1.1. Introduction

1.1.1. Zika virus

Zika virus (ZIKV) belongs to family Flaviviridae. Dengue, West Nile, yellow fever, and Japanese encephalitis viruses transmitted to humans by mosquitoes in genus Aedes all belong to family Flaviviridae. ZIKV was first isolated from a sentinel monkey in 1947 [1]. It is responsible for an unprecedented epidemic currently occurring in Brazil and the America [2]. Before this outbreak, ZIKV was not viewed as an important pathogen as majority of its infections are asymptomatic [3]. However, there is now growing evidence showing that ZIKV infections maybe linked to fetal and newborn microcephaly [4, 5] and serious neurological complications such as Guillain–Barré syndrome (GBS) [6]. Moreover, ZIKV intersects with the placenta and causes microcephaly by targeting cortical progenitor cells, inducing cell death by apoptosis and autophagy and impairing neurodevelopment [7, 8]. The increases in Guillain-Barré syndrome and microcephaly associated with ZIKA infection led World Health Organization (WHO) to declare ZIKV infection as a global public health emergency on February 1, 2016 [4, 5]. To date, no vaccine or therapeutic has been

clinically approved to prevent or control ZIKV infection.

1.1.2. Zika virus NS2B-NS3 protease

ZIKV has a single positive sense RNA genome. It is initially translated as a single polyprotein approximately 11 kb [9] and then post-translationally cleaved into three structural proteins (capsid (C), premembrane/membrane (prM), envelope (E)) and seven nonstructural (NS) proteins (NS1, NS2A, NS2B, NS3, NS4A, NS4B, and NS5) [10]. NS3 protein of ZIKV possesses putative protease activity at its N-terminus with putative ATPase/helicase, nucleoside triphosphatase, and 5'-triphosphatase activities at its C-terminus [11]. The polyprotein is cleaved co- and post- translationally by cellular proteases of furin-type or Golgi-localized proteases and the viral serine protease embedded in the N-terminal domain of NS3 ($NS3^{pro}$) [12]. Since NS3 is essential to life cycle of ZIKV, it is an attractive target for the development of antiviral drugs [13].

1.1.3. Phenolic compounds

Phenolic compounds are secondary metabolites found abundantly in a wide variety of food such as fruits, vegetables, herbs, seeds, cereals, and beverages such as coffee, tea, cocoa, and wine [14]. Natural phenolic compounds have numerous biological activities and health benefits for preventing or treating age-related diseases [15], cancers [16], and heart diseases [17]. Antiviral activities of phenolic compounds for influenza virus (A/H1N1, A/H3N2 and B virus) [18], severe acute respiratory syndrome coronavirus (SARS-CoV) [19], and dengue fever virus [20] have also been reported. However, up to date,

there has been no report on the inhibitory activity and their structure-activity relationship of phenolic compounds against NS2B-NS3^{pro} of ZIKV.

In this study, we expressed NS2B-NS3^{pro} from ZIKV in *E. coli* and studied inhibitory activities of twenty-two phenolic compounds compounds belonging to four groups (flavonol, flavanol, flavone, and flavanone) against ZIKV NS2B-NS3^{pro} as well as their structure-activity relationship. This study was published on Biotechnology Letters in 2017[44].

1.2. Materials and methods

1.2.1. Preparation of ZIKV NS2B-NS3^{pro}

ZIKV NS2B-NS3^{pro} gene was synthesized after codon optimization (Genscript, Piscataway, NJ, USA) for expression in Escherichia coli based on amino acid sequence of NS2B-NS3^{pro} (GenBank accession No. ALU33341.1) [21]. It was inserted into pET28a vector (Novagen, Darmstadt, Germany) (pET28a-NS2B-NS3^{pro}) for the expression of NS2B-NS3^{pro} enzyme with polyhistidine tags in both N-terminal and C-terminal ends(Figure 1). The protein encoding NS2B-NS3^{pro} comprised 49 NS2B amino acid residues (amino acid residues 1421-1469) linked by a flexible GGGGSGGGG linker with 186 NS3^{pro} amino acid residues (amino acid residues 1503 – 1688) (Figure 2). pET28a-NS2B-NS3^{pro} was transformed into *E. coli* BL21(DE3) which were grown in LB supplemented with kanamycin (50 μg/ml) at 37°C. Cells were induced with 0.5 mM Isopropyl β-D-1-thiogalactopyranoside (IPTG) when optical density reached 0.5. Induced cells were kept at 16°C for 12 h at 200 rpm. Cells were collected by centrifugation (8,000 x g for 30 min at 4°C), resuspended in 50 mM Tris-HCl pH 7.0, and lysed via sonication (Ultrasonic processor 250, Sonics and Materials, Inc., Newtown, USA). After centrifugation (12,000 x g for 30 min), cell lysate was loaded onto 8 ml of Ni-Agarose resin (Qiagen, Hilden, Germany). Proteins were eluted from the column with 50 mM Tris-HCl, 30 mM NaCl, 500 mM imidazole, pH 8.0. Fraction containing pure protein was pooled, concentrated, and dialyzed against 50 mM Tris-HCl pH 7.0. The concentration of protein was determined spectrophotometrically at 595 nM using Bio-Rad protein assay. Purified protein was confirmed by 12% SDS-PAGE.

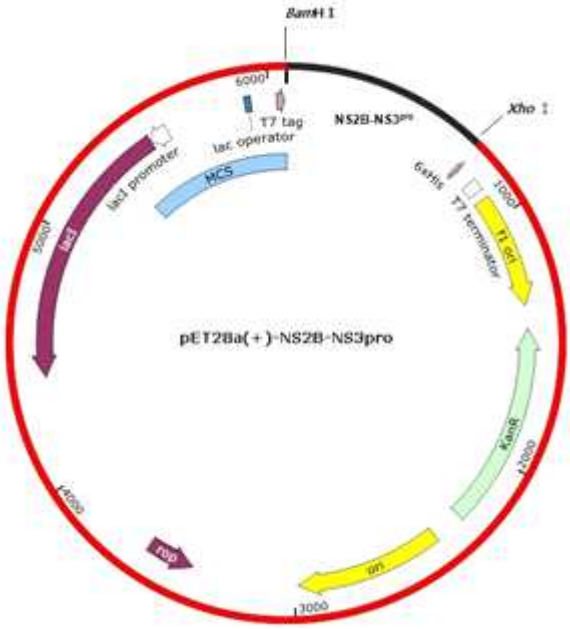

Figure 1. Vector map of pET28a-NS2B-NS3^{pro}.

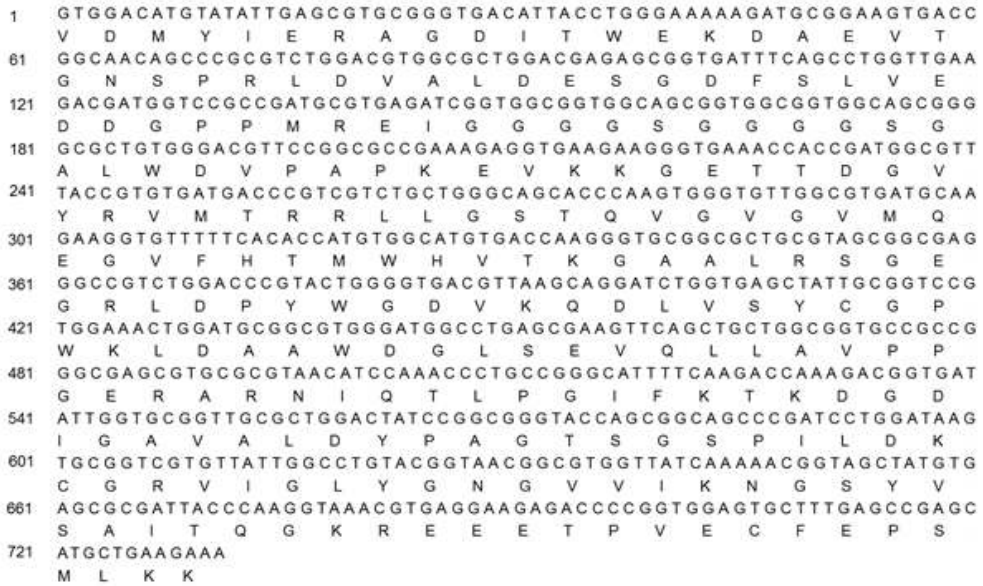

Figure 2. Nucleotide sequence of the ZIKV NS2B-NS3^{pro} gene. The codon optimized gene was synthesized based on amino acid sequence deposited at GenBank (accession No. ALU33341.1).

1.2.2. Characterization of ZIKV NS2B-NS3^{pro}

Proteolytic activity of NS2B-NS3^{pro} was measured using a fluorescence resonance energy transfer (FRET)-based assay with a substrate labeled by 5-[(2'-aminoethyl)-amino]naphthelenesulfonic acid (Edans) and 4-[[4-(dimehtylamino)phenyl]azo] benzoic acid (Dabcyl) as energy transfer pair (Bachem, Switzerland). Fluorogenic peptide Dabcyl-KTSAVLQSGFRKME-Edans was used as substrate. Enhanced fluorescence due to cleavage of this substrate catalyzed by protease was monitored at 538 nm with excitation wavelength of 355 nm using a fluorescence plate reader [19]. The reaction mixtures containing 26 μM of FRET substrate and 8.7 μg of enzyme in 50 mM Tris-HCl (pH 7.0) were run at 25°C with continuous monitoring of fluorescence for 11 min. Relative fluorescence units (RFUs) were recorded with SpectraMax M3 (Molecular Devices, USA) at excitation and fluorescence emission wavelength of 355 and 538 nm, respectively.

The effect of pH on ZIKV NS2B-NS3^{pro} enzyme activity was studied by performing assays at different pH values ranging from pH 3.0 – 11.0 using 50 mM of the following buffer: glycine-HCl (pH 3.0), sodium acetate buffer (pH 5.0 – 6.5), Tris buffer (pH 7.0 – 9.0), and glycine-NaOH buffer (pH 9.5 – 11.0). The optimum pH was assayed by incubation ZIKV NS2B-NS3^{pro} enzyme in each buffer for 15 min using 26 μM of FRET as substrate.

Kinetic parameter of NS2B-NS3^{pro} was obtained using substrate at concentration of 2.5 to 40 μM in the fluorescent assay followed by 11 min of incubation. Reaction responses were linear within this time.

Michaelis-Menten constant (K_m) was calculated from the Lineweaver-Burk plot using Sigmaplot program (Systat Software, USA).

1.2.3. Inhibition assay

Epigallocatechin gallate (EGCG) and astragalin were obtained from Amore Pacific (Yong-in, South Korea). EGCG glucosides were prepared as described previously [22]. Rutin and ampelospsin were purchased from Acros Organics (New Jersey, USA) and ZR chemicals (Shanghai, China), respectively. Others chemicals were purchased from Sigma. For initial screening, each compound was either dissolved in dimethyl sulfoxide (DMSO) or distilled water to obtain 10 mM stock solution. The reaction mixture contained 26 μM FRET substrate, 8.7 μg of enzyme, and 100 μM inhibitor in 50 mM Tris-HCl (pH 7.0). The reaction was run at 25°C for 11 min. Inhibition activity was calculated using the following equation (1):

$$\text{Inhibition activity (\%)} = 100 - [(S - So)/ (C - Co)] \times 100 \qquad (1)$$

Where C was the RFUs of the control (enzyme, buffer, and substrate) after 11 min of reaction, C_0 was the RFUs of the control at time zero, S was the RFUs of the test sample (enzyme, inhibitor, buffer, and substrate) after 11 min of reaction, and S_0 was the RFUs of the tested samples at time zero. The 50% inhibitory concentration (IC_{50}) was defined as the concentration of NS2B-NS3^{pro} inhibitor necessary to reduce NS2B-NS3^{pro} activity by 50% relative to a reaction mixture containing NS2B-NS3^{pro} enzyme without any inhibitor. Inhibitor kinetic studies were performed for myricetin with multiple

inhibitor concentrations (0-50 μM) and various substrate concentrations (10-50 μM). The inhibition type was determined using Lineweaver-Burk and Dixon plot (1/v as a function of inhibitor concentration [I]). Inhibition constant (K_i) was calculated using Sigmaplot program.

1.3. Results and discussion

1.3.1. Expression of ZIKV NS2B-NS3^{pro}

Similar to other Flavivirus proteases such as those of dengue virus (DENV) and West Nile virus (WNV), the mature form of ZIKV protease consists of the N-terminal domain of NS3, which carries the catalytic triad Ser135-His51-Asp75 and requires the central hydrophilic domain of NS2B as a co-factor for enzymatic activity [13, 23]. Its cleavage sites have common Lys-Arg, Arg-Arg, Arg-Lys, or Gln-Arg motifs [13, 24]. ZIKV NS2B-NS3^{pro} was designed to compose 49 NS2B amino acid residues (amino acid residues 1421-1469) linked by a flexible GGGGSGGGG linker with 186 NS3^{pro} amino acid residues (amino acid residues 1503 - 1688) (Figure 2). It was cloned and expressed in *E. coli* BL21(DE3). The purification of recombinant ZIKV NS2B-NS3^{pro} was achieved in a single Ni-Agarose chromatography with 21-fold purification. SDS-PAGE analyses revealed a protein band of approximately 35 kDa (Figure 3) with over 80% purity.

ZIKV NS2B-NS3^{pro} proteins were found to be able to cleave fluorogenic peptide Dabcyl-KTSAVLQSGFRKME-Edans with λ_{ex} = 355 nm and λ_{em} = 538 nm at 25°C in 50 mM Tris-HCl (pH 7.0). The maximum activity of purified ZIKV NS2B-NS3^{pro} was obtained at pH 7.0. ZIKV NS2B-NS3^{pro} showed over 80% activity at pH 6.5 to 9.5 (Figure 5).

Michaelis-Menten kinetic and Lineweaver-Burk plot for the determination of K_m are shown in Figure 4. The K_m of ZIKV NS2B-NS3^{pro} calculated from the double reciprocal Lineweaver-Burk plot was 26.3 μM.

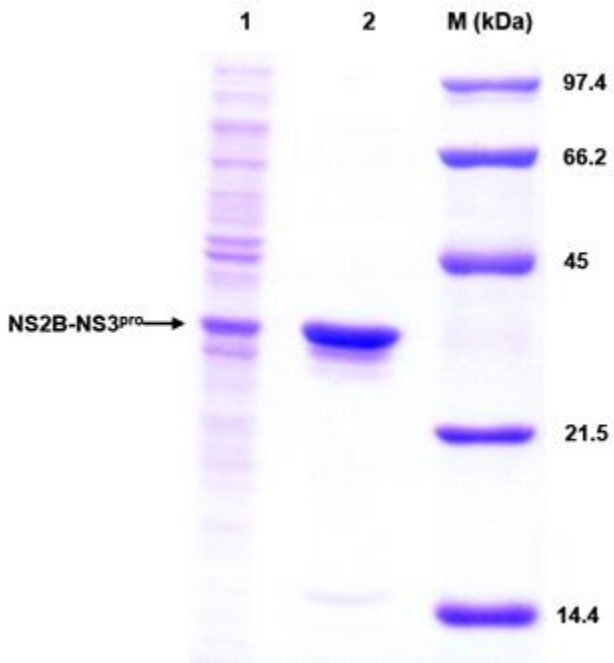

Figure 3. SDS-PAGE of the purified NS2B-NS3^{pro}.

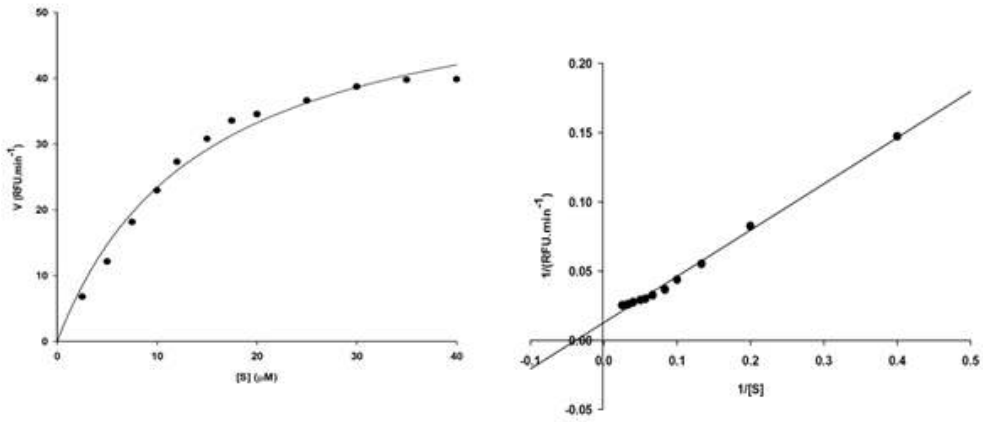

Figure 4. Michaelis-Menten kinetic and lineweaver-Burk plot of the purified NS2B-NS3^{pro}.

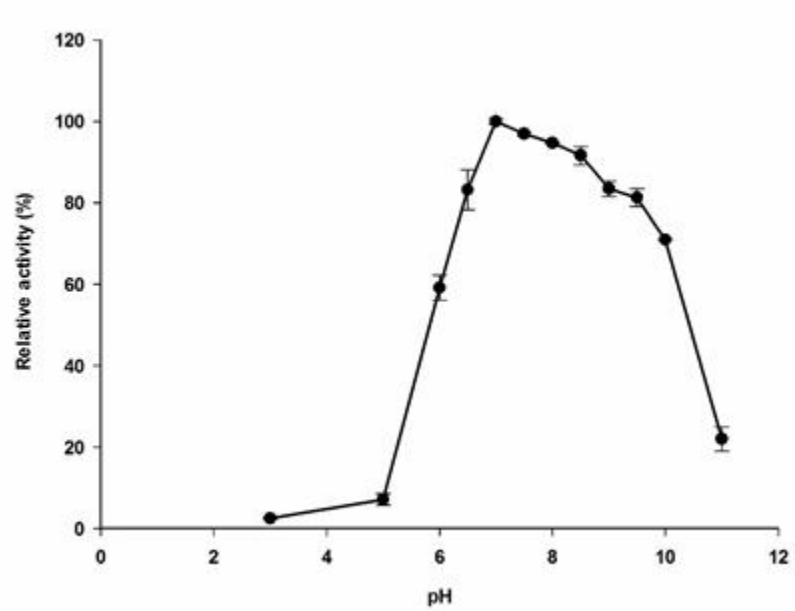

Figure 5. Effect of pH on ZIKV NS2B-NS3^{pro} activity.

1.3.2. Phenolic compounds inhibition against the activity of ZIKV NS2B-NS3^{pro}

Phenolic compounds are natural compounds ubiquitously found in plants [14]. It has been reported that phenolic compounds fisetin, quercetin, anringin, and rutin can inhibit dengue virus, a member of family Flaviviridae that also contains ZIKV [20]. Therefore, in this study, twenty phenolic compounds belonging to four groups of flavonoids (flavonol, 6 compounds; flavanol, 8 compounds, flavone, 2 compounds, flavanone, 2 compounds) and four non-flavonoid type phenolic compounds (pyrogallol, pyrocatechol, caffeic acid, and gallic acid) were selected to test their inhibitory activities against ZIKV NS2B-NS3^{pro}. The structures of these compounds are shown in Figure 7.

The inhibitory constant (*Ki*) and the half maximal inhibitory concentration (IC_{50}) of a drug that is known to cause inhibition of enzyme have to do with the concentration needed to reduce the activity of that enzyme by half. More specifically the *Ki* is reflective of the binding affinity and the IC_{50} is more reflective of the functional strength of the inhibitor, but both factor in the concentration of drug present to inhibit the enzyme activity. Therefore, the smaller the *Ki*, the smaller amount of medication needed in order to inhibit the activity of that enzyme. Result on the inhibition activities of these phenolic compounds at 100 μM against NS2B-NS3^{pro} are shown in Table 1. Among the tested compounds, myricetin, astragalin, rutin, epigallocatechin gallate, epicatechin gallate, gallocatechin gallate, and luteolin that over 40% inhibitory activities against ZIKV NS2B-NS3^{pro}. Therefore, they were selected for the determination of their IC_{50} values. Results are shown in Table 1. The IC_{50} of myricetin, astragalin, rutin, EGCG, epicatechin gallate (ECG),

gallocatechin gallate (GCG), and luteolin were 22.2 ± 0.2, 112.0 ± 5.5, 104.7 ± 2.9, 87.3 ± 1.2, 88.9 ± 1.6, 98.9 ± 1.8, and 53.0 ± 1.3 μM, respectively (Table 1 and Figure 6).

Among these tested compounds, myricetin showed the strongest inhibitory activity against ZIKV NS2B-NS3^{pro}. Therefore, it was subjected to kinetic characterization. Inhibitory kinetic experiments were performed at different constant inhibitor concentrations and various substrate concentrations. Lineweaver-Burk and Dixon plots were used to analyze the inhibition modes of these compounds. Results are shown in Figure 8. The slopes of these lines confirmed that myricetin was a mixed type of inhibitor against NS2B-NS3^{pro}. Based on linear regression analysis of the Dixon plot, the inhibitory constant (K_i) of myricetin was found to be 8.9 ± 1.9 μM.

Table 1. Inhibitory activities of the 22 phenolic compounds against NS2B-NS3^{pro}

Group	No.	Compound	Inhibition (%)	IC_{50} (μM)
Flavone	**1**	Luteolin (D[a])	54.3	53.0 ± 1.3
	2	Chrysin (D)	19.3	-
Flavonol	**3**	Myricetin (D)	87.9	22.2 ± 0.2
	4	Quercetin (D)	32.6	-
	5	Ampelopsin (D)	23.2	-
	6	Astragalin (D)	47.6	112.0 ± 5.5
	7	Rutin (D)	49.3	104.7 ± 2.9
	8	Icaritin (D)	19.3	-
Flavanone	**9**	Hesperidin (D)	7.0	-
	10	Naringin (D)	12.5	-
Flavanol	**11**	Epigallocatechin gallate (W[b])	51.5	87.3 ± 1.2
	12	Epicatechin gallate (D)	52.0	88.9 ± 1.6
	13	Gallocatechin gallate(D)	52.0	98.9 ± 1.8
	14	Catechin gallate (D)	32.1	-
	15	EGCG-7-O-α-glucopyranoside (W)	25.0	-
	16	EGCG-4'-O-α-glucopyranoside (W)	23.2	-
	17	Epigallocatechin (D)	7.0	-
	18	Catechin (D)	7.3	-
Other	**19**	Pyrogallol (W)	11.2	
	20	Pyrocatechol (W)	8.0	-
	21	Caffein (W)	6.2	-
	22	Gallic acid (W)	14.7	-

D[a]: dissolved in DMSO; W[b]: dissolved in distilled water; (-): Not determined.

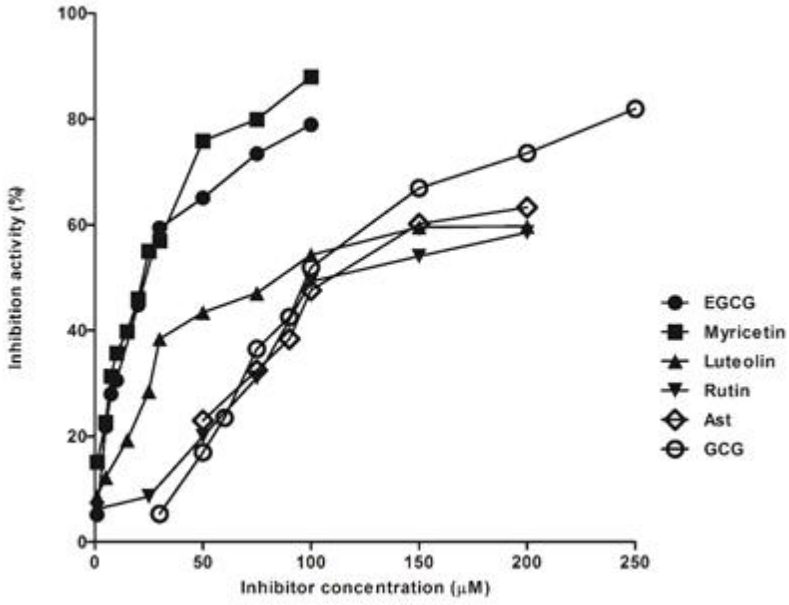

Figure 6. Inhibitory activity of 6 compounds against ZIKV NS2B-NS3^{pro}.

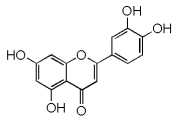

1

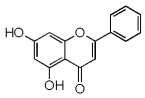

2

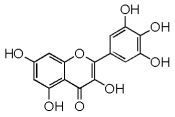

3

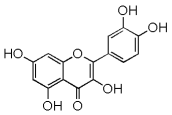

4

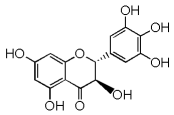

5

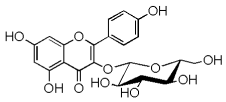

6

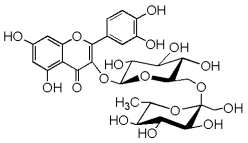

7

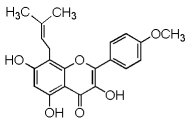

8

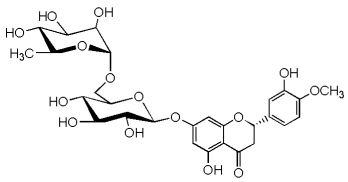

9

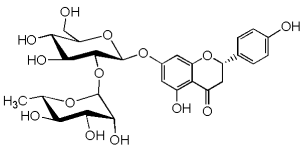

10

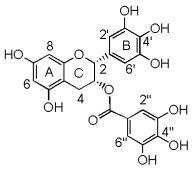

11

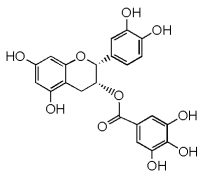

12

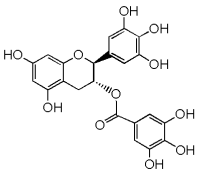

13

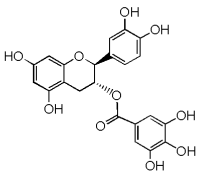

14

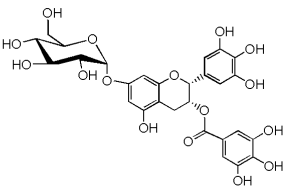

15

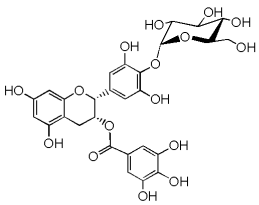

16

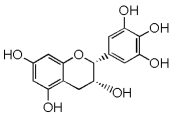

17

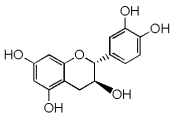

18

19

20

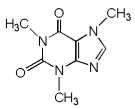

21

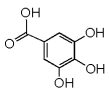

22

Figure 7. Structures of flavonoid inhibitors and others. 1: Luteolin; 2: Chrysin; 3: Myricetin; 4: Quercetin; 5: Ampelopsin; 6: Astragalin; 7: Rutin 8: Icaritin 9: Hesperidin; 10: Naringin; 11: Epigallocatechin gallate (EGCG); 12: Epicatechin gallate (ECG); 13: Gallocatechin gallate(GCG); 14: Catechin gallate (CG); Epicatechin (EC); 15: EGCG-7-O-α-glucopyranoside; 16: EGCG-4'-O-α-glucopyranoside; 17: Epigallocatechin (EGC); 18: Catechin; 19: Pyrogallol; 20: Pyrocatechol; 21: Caffeine; 22: Gallic acid.

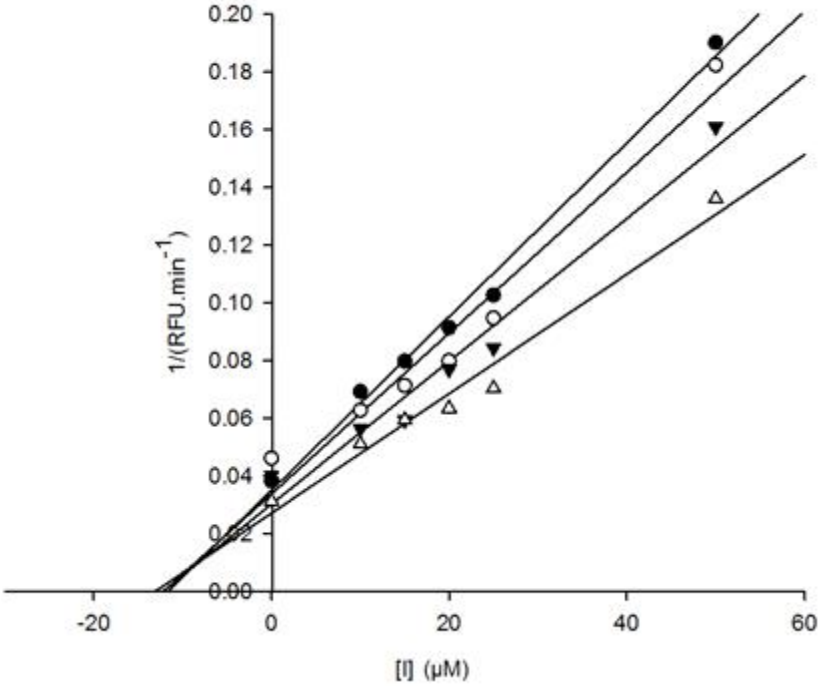

Figure 8. Dixon plot analysis of the inhibition of NS2B-NS3^{pro} by myricetin (●: 10 μM; ○: 15 μM; ▼: 25 μM; Δ: 50 μM).

1.3.3. Relationship between chemical structure of inhibitor and ZIKV NS2B-NS3^{pro} activity

In flavone class of compounds, luteolin showed 2.8 times higher inhibition activity compared to chrysin due to the presence of two OH groups at C3' and C4' in its B-ring. Myricetin, quercetin, ampelopsin, astragalin, rutin, and icaritin belong to the flavonol class of compounds. The order of their inhibitory activities was as follows: myricetin < rutin < astragalin < quercetin < ampelopsin < icaritin. Icaritin has lower inhibitory activity compared to the remaining compounds in this class. The methoxy group at C4' in B-ring and prenyl group at C8 position in the A-ring of icaritin have contributed to its lower inhibitory activity. Myricetin contains three OH groups at its B-ring. Ampelopsin has the same three OH groups at its B-ring. However, ampelopsin lacks the double bonds between the C2 and C3 positions in the C-ring. The absence of the double bonds in ampelopsin might have decreased the inhibitory activity. This might be the primarily reason why ampelopsin had lower inhibitory activity than myricetin. Quercetin had lower inhibitory activity compared to myricetin, luteolin, and astragalin. Rutin having glycosylation at C3 position in the C-ring but no OH group at C3' in the B-ring had higher inhibitory activity than quercetin, although their inhibitory activities were lower than those of myricetin and luteolin. These results suggest that the presence of OH group at C3', C4', and C5' in the B-ring is very important for the ZIKV NS2B-NS3^{pro} inhibitory activity while the absence of OH group or glycosylation at C3 position in the C-ring of flavonols only has slight effect on the ZIKV NS2B-NS3^{pro} inhibitory activity. Hesperidin and naringin belong to flavanones. They have a single bond

between the C2 and C3 positions in the C-ring. They showed weak inhibition activity against ZIKV NS2B-NS3^{pro}, indicating that bulky glycosylation at C7 in the A-ring can decrease their inhibition activity against ZIKV NS2B-NS3^{pro}. EGCG, EGCG-7-O-α-glucopyranoside, EGCG-4'-O-α -glucopyranoside, epigallocatechin, catechin gallate, catechin, ECG, and GCG belong to flavanol class of compounds. They lack the double bond (between the C2 and C3 positions) and C4 = O in C-rings. EGCG, EGCG-7-O-α -glucopyranoside, EGCG-4'-O-α-glucopyranoside, catechin gallate, ECG, and GCG containing galloyl moiety at the 3-OH position in the C-ring showed higher inhibition activity against ZIKV NS2B-NS3^{pro} than epigallocatechin and catechin. EGCG, ECG, and GCG (epimer of EGCG) showed similar inhibition activities. There was no significant difference in inhibition activity between epigallocatechin and catechin, indicating that the OH group at C5' in the B-ring does not affect their inhibition activities. EGCG-7-O-α-glucopyranoside and EGCG-4'-O-α-glucopyranoside showed lower inhibition activities than EGCG due to glycosylation at C7 position in A-ring and C4' position in B-ring, respectively.

1.4. Conclusion

In summary, we studied the inhibitory activities of twenty-two phenolic compounds against ZIKV NS2B-NS3^{pro}. Seven compounds were found to have IC_{50} from 22.2 ± 0.2 to 112.0 μM. Based on structure-activity relationship of these compounds against ZIKV NS2B-NS3^{pro}, we found that double bonds between C2 and C3 in the C-ring, OH groups at C7 in the A-ring, C3', C4', and C5' in the B-ring, and galloyl moiety at C3 in the C-ring all played an important role in the inhibition activity against ZIKV NS2B-NS3^{pro}. These relationships between chemical structures and activities against ZIKV NS2B-NS3^{pro} can be further explored to develop highly selective inhibitors against ZIKV NS2B-NS3^{pro}.

Chapter 2. Production of rubusoside from stevioside using β-galactosidase from *Thermus thermophilus*

2.1. Introduction

2.1.1. Steviol glycosides

Steviol glycosides are extracted from the *Stevia Rebaudiana* (bertoni) commercially cultivated in many countries[25]. Because of their high sweetness, lower calorific value and many biological effects, steviol glycosides have caused great interest in some researchers and food additive producers[26]. Stevioside(Ste, 13-[(2-O-β-D-Glucopyranosyl-α -D-glucopyranosyl)oxy]kaur-16-en-18-oic acid β-D-glucopyranosyl ester) is a main component of Steviol glycosides. It tastes about 300 times sweeter than sucrose. Other compounds present but in lower concentration are: steviolbioside, rebaudioside A, B, C, D, E, F and dulcoside E[27]. Rubusoside (Ru, 13-O-β-glycosyl-19-O-β-D-glucosyl-steviol) is one of steviol glycosides and it tastes about 115 times sweeter than sucrose. It was already known for enhancing solubility in water [28, 29]. Ru existed in Extract of Chinese sweet tea plant [30, 31] (*Rubus suavissimus* S. Lee; known in Japan as Tenryocha or Tencha [32]). The tea plant grows only in southern China with variable yearly yields depending on local climate [33], and large scale purification of Ru is complicated[34]. Ste has three β-glycosidic bonds (β-linked sophorose, β-1,2-D-glucopyranosyl on C13 and an ester β-glucosidic linkage on the C19 carboxyl group)[35]. Thus, selective cleavage of β-1,2-glucosidic linkage of sophorosyl moiety at C13 of Ste can produce Ru.

2.1.2 β-galactosidase from *Thermus thermophilus*

β-galactosidase is known as lactase which hydrolyses lactose into glucose and galactose. It is one of the most important enzymes used to produce low-lactose or lactose-free products as a response to lactose intolerance of consumers, which affects approximately 70% of the world population[36]. In previous studies, it was already reported that β-galactosidase from *Aspergillus* spp.[33], β-glucosidase form *Aspergillus aculeatus*[34] and *Streptomyces* sp. GXT6[37] can hydrolyze Ste into Ru. The Ru production yields of these enzymes were 91.4%, 52% and 78.8%, respectively. However, in previous another study[35], it was reported that β-galactosidase from *Thermus thermophilus* was thermostable at 100°C and its Ru production yield was 86%.

2.1.3 Immobilization of enzyme

Immobilization is important to maintain constant environmental conditions in order to protect the enzyme against changes in pH, temperature, or ionic strength; this is generally reflected in enhanced stability[38]. Moreover, immobilized enzymes can be more easily separated from substrates and reaction products and used repeatedly. Many different procedures have been developed for enzyme immobilization; these include adsorption to insoluble materials, entrapment in polymeric gels, encapsulation in membranes, crosslinking with a bifunctional reagent, or covalent linking to an insoluble carrier[39]. Entrapment, one of the immobilization techniques, can be defined as physical restriction of enzyme within a confined space or network. Gelation of polyanionic or polycationic polymers by the addition of

multi-valent counter-ions is a simple and common method of enzyme entrapment. Alginates are one of the most frequently used polymers due to their mild gelling properties and non-toxicity. Alginate is an anionic linear copolymer composed of 1,4′-linked β-d-mannuronic acid and α-l-guluronic acid in different proportions and sequential arrangements[40]. Enzymes are entrapped by drop-wise addition of an aqueous solution of sodium alginate and the biocatalyst to a hardening solution of a Ca2+ salt. The cation acts a cross-linking agent towards the alginate biopolymer and the droplets precipitate as beads with the biocatalysts entrapped within the network[41].

In this study, to produce Ru effectively, the expression of β-galactosidase from *T. thermophilus* was optimized with different *E. coli* hosts and with different concentrations of lactose inducer rather than isopropyl-1-β-D-thiogalactopyranoside (IPTG) for industrial production of the enzyme. And then, for industrialization of production of Ru, the reaction was carried out in the vertical double-jacket glass column reactors thermostatted at 70°C. This study was published on Functional Food in Health and Disease in 2016[45].

2.2. Materials and methods

2.2.1. Chemicals

Ste was purchased from DAEPYUNG. Ru standard was prepared as our previous reported[35]. Other chemicals were purchased from Sigma and other companies.

2.2.2. Selection of expression strains

The β-galactosidase gene, β-glypi, was ligated into the *Xho*I/*Eco*RI-digested pRSETB (pRSETB-β-GLYPI) vector as described in the previous study. pRSETB-β-GLYPI was transformed and expressed in *E. coli* BL21(DE3)pLysS, *E. coli* Rosetta(DE3)pLysS, and *E. coli* BL21(DE3). Cells were grown in 100 ml LB media containing 0.5% (w/v) yeast extract, 1.0% (w/v) tryptone, 1.0% (w/v) NaCl, and supplemented with ampicilin (50 μg/ml) in 500 ml flasks at 37°C. The cells were induced with 7 mM lactose when the optical density reached (OD_{600}) 0.5 with 15 h of shaking. The cells were collected by centrifugation (8000 x g for 30 min at 4°C), resuspended in 50 mM Tris-HCl pH 7.0, and then lysed via sonication (Ultrasonic processor 250, Sonics and Materials, Inc., Newtown, CT, USA; output 30, for 1 min, 4 repeat on ice). After centrifugation (12,000 x g for 30 min), the clarified cell lysate was checked for enzyme activity using lactose as the substrate.

2.2.3. Optimization of lactose concentration for induction

E. coli BL21(DE3)pLysS was selected to determine the effect of lactose concentration for enzyme expression. The induction was carried out as described above with varying concentrations of lactose for induction (1 ~ 7

mM) at 37°C for 15 h.

2.2.4. β-galactosidase hydrolytic activity assay

The hydrolytic activity was determined using lactose as a substrate. The reaction mixture containing 200 mM lactose and enzyme in 50 mM Tris-HCl pH 7.0 was reacted at 70°C for 20 min. The mixture was analyzed by thin layer chromatography (TLC) using precoated silica gel 60 F254 plates (Merck, Darmstadt, Germany) developed in a solvent system consisting of acetonitrile:water [85:15 (v/v)]. The plates were visualized by dipping into a solvent mixture of 0.5% (w/v) N-(1-naphthyl) ethylenediamine dihydrochloride and 5% (w/v) sulfuric acid in methanol and heating at 120°C for 10 min. The concentration of glucose released by β-galactosidase was analyzed using the integrated density values (IDV) derived by the AlphaEaseFC 4.0 program (Alpha Inotech, San Leandro, CA, USA) with glucose standard. One unit (U) of galactosidase activity is defined as the amount of enzyme required to release 1 μmol glucose per minute under the above reaction conditions.

2.2.5. Fermentation and purification of β-galactosidase

Large scale production of β-galactosidase was carried out in 19 L fermenter (Bioengineering AG., Riki, Switzerland) that contained 14 L LB media. The fermentation conditions were 37oC, 250 rpm, and an aeration rate of 2 vvm. Cells were grown at 37oC until OD600 reached 0.6, at which point 5 mM lactose was added; the cells were harvested after 15 h. The cells were collected by centrifugation (7,871 x g for 30 min at 4°C), re-suspended in 500 ml of 50 mM Tris-HCl pH 7.0, and disrupted by

sonication. The clarified cell lysate was obtained after centrifugation for 30 min at 12,000 x g and partially purified β-galactosidase was heat treated at 70°C for 15 min. Heat-denatured proteins were removed by centrifugation at 8,000 x g for 15 min. The supernatant was freeze dried for further study. The protein concentration was determined by the Bradford method with crystalline bovine serum albumin as the standard.

2.2.6. Immobilization of β-galactosidase

β-galactosidase was mixed with 2.5% (w/v) sodium alginate solution to give final unit 300 unit/ml of sodium alginate bead. The mixture obtained was extruded drop-wise through a mini-pump variable flow(Fisher Scientific, Waltham, MA, USA) into 3% (w/v) CaCl2•2H2O with gentle stirring for 30 min to obtain a bead size of 2 mm. The calcium alginate beads containing the enzyme were thoroughly washed with distilled water, kept in 3% (w/v) CaCl2•2H2O solution for stabilizing for 30 min, and rewashed with distilled water, then kept at 4°C for 2 h.

2.2.7. Production of Rubusoside mixture using double jacket columns

The double jacket column reactors [Condenser, Liebig, with joint, 30 x 3 (cm) in diameter] were filled with β-galactosidase beads. The reaction temperature was controlled using a heat circulator (EYELA, NCB-1200, Tokyo, Japan) at 70°C. The reaction mixture containing 0.5% of Ste solution was pumped into the columns using a mini pump at the speed of 0.01 ml per min for 45 g Ste per day. The reaction mixture passed through columns and the fractions were collected into Eppendorf tubes. The Ru mixture was

analyzed by TLC measuring integrated density values (IDV) derived from the AlphaEaseFC 4.0 program (Alpha Inotech, San Leandro, CA, USA) with purified Ru as the standard.

2.2.8. Purification of rubusoside

Ru was purified as previously reported [35] by using Reveleris® Amino 120 g Flash Cartridges (Grace Discovery Science, Shanghai, China) with an evaporative light scattering detector (ELSD, Grace Discovery Science, Shanghai, China). A mixture of acetonitrile and water was used as an eluent with the gradient from 99:1 (v/v) to 50:50 (v/v) of acetonitrile: water at a flow rate of 60 ml/min at room temperature. The purified Ru was collected and freeze dried for further study.

2.3. Results and discussion

2.3.1. Optimization for the expression of β-galactosidase

Table 2 shows the β-galactosidase activity from *T. thermophilus* expressed in *E. coli* BL21(DE3)pLysS, *E. coli* Rosetta(DE3)pLysS, and *E. coli* BL21(DE3) at 28°C or 37°C. The expressed β-galactosidase activity was 34.3, 14.2, or 34.4 ± 0.5 U/ml in *E. coli* BL21(DE3)pLysS, *E. coli* Rosetta(DE3)pLysS, or *E. coli* BL21(DE3) at 37°C, and 9.8 ± 0.2, 7.0 ± 0.5, or 7.4 ± 0.2 U/ml at 28°C, respectively. The β-galactosidase activity at 37°C induction was 3.5 fold greater in *E. coli* BL21(DE3)pLysS expression, 2.0 fold greater in *E. coli* Rosetta(DE3)pLysS expression, and 4.7 fold greater in *E. coli* BL21(DE3) expression than those at 28°C induction. The *E. coli* BL21(DE3)pLysS was selected for the investigation of the lactose concentration effect of the β-galactosidase expression (Figure 9) based on the similarity in β-galactosidase activity expressed in *E. coli* BL21(DE3)pLysS and *E. coli* BL21(DE3). β-galactosidase activity was increased from 19.1 ± 0.7 U/ml to 53.3 ± 1.5 U/ml when the concentration of lactose inducer was increased from 1 to 5 mM. For lactose induction concentrations above 5 mM, the β-galactosidase activity expressed was decreased to 48.4 ± 1.7 mM. Hence, the selected lactose concentration for induction was 5 mM.

Table 2. β-galactosidase activity expressed from different *E. coli* at 7 mM lactose induction

Temperature	***E. coli*** **BL21(DE3)pLysS (U/mL)**	***E. coli*** **Rosetta(DE3)pLysS (U/mL)**	***E. coli*** **BL21 (DE3) (U/mL)**
28°C	9.8 ± 0.2	7.0 ± 0.5	7.4 ± 0.2
37°C	34.3 ± 0.0	14.2 ± 0.3	34.4 ± 0.5

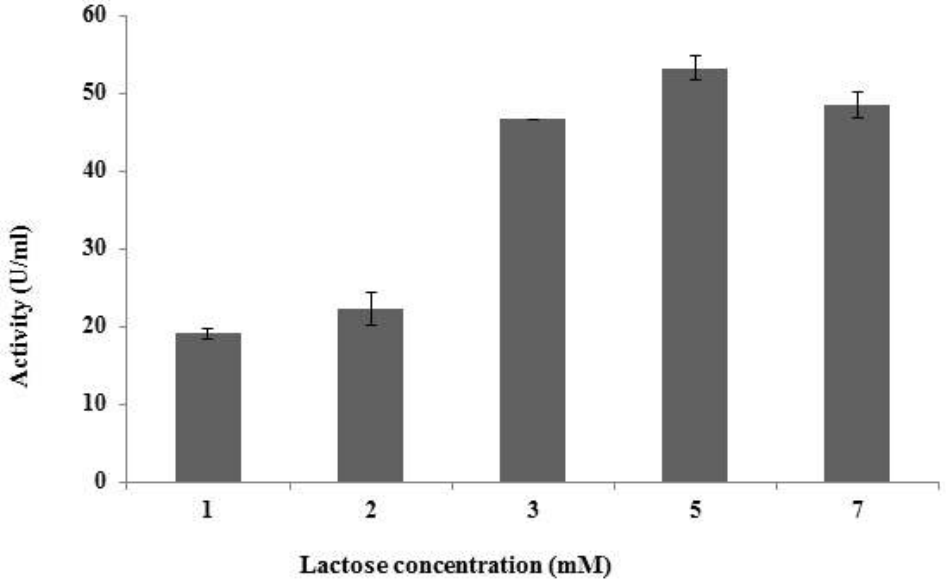

Figure 9. β-galactosidase activity expressed from *E. coli* BL21(DE3)pLysS with lactose induction

2.3.2. Fermentation of recombinant β-galactosidase

Compared to mesophilic enzymes, thermostable enzymes exhibiting maximal activity at temperatures ranging from 70 to 90°C have significant advantages, including greater reaction velocity, reduced risk of microbial contamination, and longer enzyme half-lives under operational conditions [42, 43]. After the heating of crude β-galactosidase solution, 78% of the mesophilic proteins were eliminated with 89% β-galactosidase activity recovery (Table 3). The partially purified β-galactosidase demonstrated a specific activity of 23 U/mg corresponding to a 4-fold purification.

Table 3. Partial purification of β-galactosidase

	Total volume (mL)	**Total protein (mg)**	**Total unit (U)**	**Specific activity (U/mg)**	**Purification (fold)**	**Yield (%)**
Crude enzyme	2,000	35,814.9	204,000	5.7	1	100
After Heat treatment	1,650	7,885.0	181,500	23.0	4	89.0

2.3.3. Production of rubusoside using immobilized β-galactosidase on double jacket columns

The free enzyme reaction was carried out by mixing 0.5% (w/v) Ste and 300 U/ml in 50 mM Tris-HCl pH 7.0 at 70°C in a water bath for 12 h. By using free enzyme, the amount of Ru produced was 3.3 g/L and the Ste conversion was 74.3% (Table 4). For the double jacket column, the reaction was carried for 31 days. The amount of Ru released from Ste is shown in Table 4. The total amount of Ru produced was 738.7 g for 31 days. Immobilized enzyme demonstrated 77% activity up to 21 days and then the activity gradually reduced in the span of 31 days, while still maintaining 51.4% β-galactosidase activity (Table 5). 1395 g of Ste was used for reaction. The yield of Ru produced was 53.0%.

Table 4. Conversion from Ste to Ru using immobilized enzyme and free enzyme

	Amount of Ste hydrolysis (g/L)	Conversion (%)*	Amount of Ru production (g/L)
Free enzyme	4.5 ± 0.0	74.3 ± 0.7	3.3 ± 0.0
Immobilized enzyme	4.5 ± 0.0	78.3 ± 0.7	3.5 ± 0.0

*Conversion : Ste hydrolysis/Ru production*100, The theoretical maximum conversion was 80%.

Table 5. Stability of the immobilized enzyme during double jacket columns reaction

Day*	The amount of Ru production** (g/day)	Immobilized enzyme stability (%)
6	31.3 ± 5.3	100
8	26.7 ± 8.6	85.1
11	28.9 ± 3.5	92.3
12	26.1 ± 6.1	83.3
14	24.4 ± 6.0	77.9
16	25.5 ± 0.1	81.4
19	27.4 ± 3.1	87.3
21	24.4 ± 3.0	78.0
22	18.1 ± 0.9	57.9
28	16.9 ± 3.2	54.0
29	17.1 ± 0.1	54.5
31	16.1 ± 1.4	51.4

*The reaction was carried on for 1 month.

**45 g of Ste was totally used per day. The theoretical maximum amount of Ru production was 36 g per day.

2.4. Conclusion

The expression of β-galactosidase from *T. thermophilus* was optimized using different *E. coli* hosts and a different concentration of lactose inducer rather than isopropyl-1-thio-β-D-galactopyranoside (IPTG) for industrial production of the enzyme. *E. coli* BL21(DE3)pLysS was selected for β -galactosidase from *Thermus thermophilus* expression. Lactose concentration effected for the expression of β-galactosidase and the highest activity obtained was 5 mM lactose in *E. coli* BL21(DE3)pLysS, 53.3 ± 1.5 U/mL. 78% of the mesophilic proteins was eliminated by heating at 70°C for 15 min with 89% β-galactosidase activity recovery. Immobilized enzyme was showed over 77% activity until to 21 days and then the activity was reduced and up to 31 days, β-galactosidase still remained up to 51.4% activity.

References

1. Faye, O., et al., Molecular evolution of Zika virus during its emergence in the 20th century. International Journal of Infectious Diseases, 2014. 21: p. 2-3.

2. Campos, G.S., A.C. Bandeira, and S.I. Sardi, Zika Virus Outbreak, Bahia, Brazil. Emerging Infectious Diseases, 2015. 21(10): p. 1885-1886.

3. Duffy, M.R., et al., Zika virus outbreak on Yap Island, Federated States of Micronesia. N Engl J Med, 2009. 360(24): p. 2536-43.

4. ECDC, Zika virus disease epidemic: potential association with microcephaly and Guillain–Barré syndrome (fourth update). European Center for disease Prevention and Control, 2016. fourth update: p. 18.

5. WHO, WHO statement on the first meeting of the International Health Regulations (2005) (IHR 2005) Emergency Committee on Zika virus and observed increase in neurological disorders and neonatal malformations. WHO, 2016.

6. Petersen, E., et al., Rapid Spread of Zika Virus in The Americas - Implications for Public Health Preparedness for Mass Gatherings at the 2016 Brazil Olympic Games. International Journal of Infectious Diseases, 2016. 44: p. 11-15.

7. Cugola, F.R., et al., The Brazilian Zika virus strain causes birth defects in experimental models. Nature, 2016.

8. Li, C., et al., Zika Virus Disrupts Neural Progenitor Development and Leads to Microcephaly in Mice. Cell Stem Cell, 2016.

9. Kuno, G. and G.-J. Chang, Full-length sequencing and genomic characterization of Bagaza, Kedougou, and Zika viruses. Archives of virology,

2007. 152(4): p. 687-696.

10. Baronti, C., et al., Complete coding sequence of zika virus from a French polynesia outbreak in 2013. Genome Announc, 2014. 2(3).

11. Zhu, Z., et al., Comparative genomic analysis of pre-epidemic and epidemic Zika virus strains for virological factors potentially associated with the rapidly expanding epidemic. Emerg Microbes Infect, 2016. 5: p. e22.

12. Bollati, M., et al., Structure and functionality in flavivirus NS-proteins: perspectives for drug design. Antiviral Res, 2010. 87(2): p. 125-48.

13. Lei, J., et al., Crystal structure of Zika virus NS2B-NS3 protease in complex with a boronate inhibitor. Science, 2016.

14. Vinson, J.A., et al., Phenol antioxidant quantity and quality in foods: fruits. J Agric Food Chem, 2001. 49(11): p. 5315-21.

15. Levites, Y., et al., Green tea polyphenol (-)-epigallocatechin-3-gallate prevents N-methyl-4-phenyl-1,2,3,6-tetrahydropyridine-induced dopaminergic neurodegeneration. J Neurochem, 2001. 78(5): p. 1073-82.

16. Zhao, X., et al., Apoptosis inducing effects of Kuding tea polyphenols in human buccal squamous cell carcinoma cell line BcaCD885. Nutrients, 2014. 6(8): p. 3084-100.

17. Santhakumar, A.B., et al., Consumption of anthocyanin-rich Queen Garnet plum juice reduces platelet activation related thrombogenesis in healthy volunteers. Journal of Functional Foods, 2015. 12: p. 11-22.

18. Liu, A.L., et al., Structure-activity relationship of flavonoids as influenza virus neuraminidase inhibitors and their in vitro anti-viral activities. Bioorg Med Chem, 2008. 16(15): p. 7141-7147.

19. Nguyen, T.T.H., et al., Flavonoid-mediated inhibition of SARS coronavirus

3C-like protease expressed in *Pichia pastoris*. Biotechnology letters, 2012. 34(5): p. 831-838.

20. Zandi, K., et al., In vitro antiviral activity of Fisetin, Rutin and Naringenin against Dengue virus type-2. Journal of Medicinal Plants Research, 2011. 5(23): p. 5534-5539.

21. Cunha, M.S., et al., First complete genome sequence of Zika virus (Flaviviridae, Flavivirus) from an autochthonous transmission in Brazil. Genome announcements, 2016. 4(2): p. e00032-16.

22. Moon, Y.-H., et al., Synthesis, structure analyses, and characterization of novel epigallocatechin gallate (EGCG) glycosides using the glucansucrase from *Leuconostoc mesenteroides* B-1299CB. Journal of agricultural and food chemistry, 2006. 54(4): p. 1230-1237.

23. Falgout, B., et al., Both nonstructural proteins NS2B and NS3 are required for the proteolytic processing of dengue virus nonstructural proteins. Journal of virology, 1991. 65(5): p. 2467-2475.

24. Bessaud, M., et al., Functional characterization of the NS2B/NS3 protease complex from seven viruses belonging to different groups inside the genus *Flavivirus*. Virus Res, 2006. 120(1-2): p. 79-90.

25. Upreti, M., et al., Solubility enhancement of steviol glycosides and characterization of their inclusion complexes with gamma-cyclodextrin. International journal of molecular sciences, 2011. 12(11): p. 7529-7553.

26. Huang, X.-Y., J.-F. Fu, and D.-L. Di, Preparative isolation and purification of steviol glycosides from *Stevia rebaudiana* Bertoni using high-speed counter-current chromatography. Separation and Purification Technology, 2010. 71(2): p. 220-224.

27. Kennelly, E., Sweet and non-sweet constituents of *Stevia rebaudiana* (Bertoni) Bertoni. Stevia, the Genus Stevia. Medicinal and Aromatic Plants—Industrial Profiles, 2002. 19: p. 68-85.

28. Liu, D. and Z. Chen, The effect of curcumin on breast cancer cells. Journal of breast cancer, 2013. 16(2): p. 133-137.

29. Zhang, F., et al., Reformulation of etoposide with solubility-enhancing rubusoside. International journal of pharmaceutics, 2012. 434(1): p. 453-459.

30. Koh, G.Y., G. Chou, and Z. Liu, Purification of a water extract of Chinese sweet tea plant (Rubus suavissimus S. Lee) by alcohol precipitation. Journal of agricultural and food chemistry, 2009. 57(11): p. 5000-5006.

31. Koh, G.Y., et al., Improvement of obesity phenotype by Chinese sweet leaf tea (Rubus suavissimus) components in high-fat diet-induced obese rats. Journal of agricultural and food chemistry, 2010. 59(1): p. 98-104.

32. Sugimoto, N., et al., Analysis of rubusoside and related compounds in tenryocha extract sweetener. JOURNAL-FOOD HYGIENIC SOCIETY OF JAPAN, 2002. 43(4): p. 250-253.

33. Tao, G.-j., D. Kim, and Y.-m. Xia, Enzymatic preparation of a natural sweetener rubusoside from specific hydrolysis of stevioside with β -galactosidase from *Aspergillus* sp. Journal of Molecular Catalysis B: Enzymatic, 2012. 82: p. 12-17.

34. Ko, J.-A., et al., Mass production of rubusoside using a novel stevioside-specific β-glucosidase from *Aspergillus aculeatus*. Journal of agricultural and food chemistry, 2012. 60(24): p. 6210-6216.

35. Nguyen, T.T.H., et al., Production of rubusoside from stevioside by using a thermostable lactase from *Thermus thermophilus* and solubility enhancement

of liquiritin and teniposide. Enzyme and microbial technology, 2014. 64: p. 38-43.

36. Lomer, M., G. Parkes, and J. Sanderson, Review article: lactose intolerance in clinical practice–myths and realities. Alimentary pharmacology & therapeutics, 2008. 27(2): p. 93-103.

37. Wang, Z., et al., Selective production of rubusoside from stevioside by using the sophorose activity of β-glucosidase from *Streptomyces* sp. GXT6. Applied Microbiology and Biotechnology, 2015. 99(22): p. 9663-9674.

38. Cheetham, P., Principles of industrial enzymology: Basis of utilization of soluble and immobilized enzymes in industrial processes. Handbook of enzyme biotechnology/editor, Alan Wiseman, 1985.

39. Klibanov, A.M., Immobilized enzymes and cells as practical catalysts. Science, 1983. 219(4585): p. 722-727.

40. Ertesvåg, H. and S. Valla, Biosynthesis and applications of alginates. Polymer Degradation and Stability, 1998. 59(1-3): p. 85-91.

41. Won, K., et al., Optimization of lipase entrapment in Ca-alginate gel beads. Process biochemistry, 2005. 40(6): p. 2149-2154.

42. Petzelbauer, I., et al., Development of an ultra-high-temperature process for the enzymatic hydrolysis of lactose. I. The properties of two thermostable beta-glycosidases. Biotechnology and Bioengineering, 1999. 64(3): p. 322-332.

43. Maciunska, J., M. Scibisz, and J. Synowiecki, Stability and properties of a thermostable beta-galactosidase immobilized on chitin. Journal of Food Biochemistry, 2000. 24(4): p. 299-310.

44. Lim, H.-j., et al., Inhibitory effect of flavonoids against NS2B-NS3 protease of ZIKA virus and their structure activity relationship. Biotechnology

Letters, 2016: p. 1-7.

45. Lim, H.-j., et al., Enhancement of water soluble wheat bran polyphenolic compounds using different steviol glucosides prepared by thermostable β -galactosidase. Functional Foods in Health & Disease, 2016. 6(10).

Abstract in Korean

본 연구에서는 지카 바이러스 NS2B-NS3 프로테이즈를 저해하는 페놀화합물의 저해 활성과 그들의 구조적 연관성을 확인하기 위해 35 kDa의 ZIKV NS2B-NS3 프로테이즈를 *E. coli* BL21(DE3)에서 발현하였다. fluorogenic peptide인 Dabcyl-KTSAVLQSGFRKME-Edan를 기질로 활용하여 효소의 K_m 값이 26.3 μM 으로 나타내었다. 또한 ZIKV NS2B-NS3 프로테이즈를 정제하였고, 22가지의 페놀화합물에 대한 inhibition assay와 kinetic assays를 진행하였다. 페놀화합물은 ZIKV NS2B-NS3 프로테이즈 저해 활성이 6.2% 에서 87.9% 까지 나타내었다. 7가지 페놀화합물의 IC_{50}는 22.2 ± 0.2 에서 112.0 ± 5.5 μM 까지 나타내었다. 그 중 Myricetin은 mixed type의 저해 패턴을 보였고, IC_{50}는 22.2 ± 0.2 μM, K_i 값은 8.9 ± 1.9 μM 를 보였다. 페놀화합물간의 구조적 연관성은 ZIKV NS2B-NS3의 저해제를 개발하는데 사용될 것으로 기대된다.

수용성은 인체 내에서 생체이용가능성의 중요한 역할을 한다. 루부소사이드는 스테비올 배당체 감미료중 하나로, 물속에서 수용성을 증가시키는 것으로 널리 알려져 있다. 스테비오사이드도 스테비올 배당체 감미료중 하나로, 중국의 특정 지역에서만 재배되는 루부소사이드와는 달리 다양한 나라에서 상업적으로 재배되고 있다. *Thermus thermophilus*로부터 유래한 β-galactosidase는 스테비오사이드의 β-1,2 결합을 자르는 활성을 가지고 있어, 스테비오사이드로부터 루부소사이드를 효소적으로 전환할 수 있다. 본 연구에서는, 루부소사이드의 생산을 산업화하기 위해서, 먼저, *T. thermophilus*로부터 유래한 β-galactosidase를 락토오즈 인덕션을 사용하여 *E. coli* BL21(DE3)plysS에서 발현하였다. 효소 고정화는 효소 반응을 하기에 몇 가지 장점을 가지고 있다. 고정화 효소는 특별한 분리 과정 없이

재사용이 가능하고, 활성의 저하가 크게 관찰되지 않는다. 알긴산 나트륨은 효소 고정화에 쓰이는 물질 중 하나이다. 자유 효소와 고정화 효소를 사용한 스테비오사이드 전환율은 77% 이상을 나타냈다. 효소 반응은 이중 자켓컬럼을 이용하여 70°C에서 계속적인 반응으로 진행하였다. 고정화 효소는 31일까지 안정했으며, 31일 후 51.4%의 활성이 남아있었음을 알 수 있었다.